Quaternary Science Reviews 80 (2013) 129–142

Contents lists available at ScienceDirect

Quaternary Science Reviews

journal homepage: www.elsevier.com/locate/quascirev

Moisture and temperature changes associated with the mid-Holocene *Tsuga* decline in the northeastern United States

Jeremiah P. Marsicek [a,*], Bryan Shuman [a], Simon Brewer [b], David R. Foster [c], W. Wyatt Oswald [d]

[a] Department of Geology & Geophysics, University of Wyoming, Dept. 3006, 1000 E. University Ave., Laramie, WY 82071, USA
[b] Department of Geography, University of Utah, 260 S. Central Campus Dr., Rm. 270, Salt Lake City, UT 84112, USA
[c] Harvard Forest and Department of Organismic and Evolutionary Biology, Harvard University, 324 North Main St., Petersham, MA 01366, USA
[d] Department of Communication Sciences and Disorders, Emerson College, 120 Boylston St., Boston, MA 02116, USA

ARTICLE INFO

Article history:
Received 28 February 2013
Received in revised form
31 August 2013
Accepted 3 September 2013
Available online

Keywords:
Lake levels
Hemlock (*Tsuga canadensis*) decline
Fossil pollen
Climatic change
Abrupt change
Holocene
Northeastern U.S.

ABSTRACT

A decline of hemlock (*Tsuga*) populations at ca 5.5 ka (thousands of calibrated radiocarbon years before 1950 AD) stands out as the most abrupt vegetation change of the Holocene in North America, but remains poorly understood after decades of study. Recent analyses of fossil pollen have revealed a concurrent, abrupt oak (*Quercus*) decline and increases in the abundance of beech (*Fagus*) and pine (*Pinus*) on Cape Cod in eastern Massachusetts, but the replacement of drought-tolerant oaks by moisture-sensitive beeches appears inconsistent with low lake levels in the region at the same time. The oak and beech changes are also limited to coastal areas, and the coastal-inland differences require an explanation. Here, we develop a new lake-level reconstruction from Deep Pond, Cape Cod by using a transect of sediment cores and ground-penetrating radar (GPR) profiles to constrain the past elevations of the sandy, littoral zone of the pond. The reconstruction shows that a series of multi-century episodes of low water coincide with the abrupt hemlock and oak declines, and interrupt subsequent phases of hemlock recovery. The lake-level variations equal precipitation deficits of ~100 mm superimposed on a Holocene long moisture increase of >400 mm. However, because moisture deficits do not easily explain the oak and beech changes, we also evaluate how the climate preferences of the regional vegetation changed over time by matching the fossil pollen assemblages from Deep Pond with their modern equivalents. Reconstructions of the precipitation requirements of the vegetation correlate well even in detail with the lake-level record ($r = 0.88$ at Deep Pond), and indicate close tracking of effective moisture (precipitation minus evapotranspiration) by the vegetation despite the abrupt species declines, which could have decoupled climate and vegetation trends. Reconstructions of the temperature preferences of the vegetation indicate that coastal sites may have cooled by 0.5–2.5 °C after ca 5.5 ka, while inland sites warmed by 0.5–1 °C. The change in coastal temperature preferences agrees with sea surface cooling in the western Atlantic Ocean of >1 °C. Consequently, the persistence of low hemlock abundance after 5.5 ka in the northeast U.S. may have resulted from oceanic changes that produced multi-century droughts and thus delayed the post-decline recovery of hemlock populations.

1. Introduction

Davis (1981) described an abrupt hemlock (*Tsuga* spp.) decline across eastern North America at ca 5.5 ka (thousands of calibrated radiocarbon years before 1950 AD), noting sharp decreases in hemlock pollen abundances from Michigan to Maine. The decline was initially attributed to a pathogen or pest outbreak because of 1) the range-wide abrupt nature of the decline, 2) the apparent change in only one taxon, 3) the similarity of the event's palynological signature to recent forest disease outbreaks, and 4) a lack of evidence for concurrent climate change or other drivers (Allison et al., 1986). The change, therefore, appeared to represent an abrupt ecological event independent of progressive Holocene climate changes. Since then, additional work has linked the decline to insect outbreaks (Anderson et al., 1986; Bhiry and Filion, 1996), dated the mid-point of the regional decline to 5.5 ± 0.38 ka

* Corresponding author. Tel.: +307 703 0747; fax: +307 766 6679.
E-mail address: jmarsice@uwyo.edu (J.P. Marsicek).

0277-3791/$ – see front matter
http://dx.doi.org/10.1016/j.quascirev.2013.09.001

(Bennett and Fuller, 2002), and documented the decline as one of the most abrupt vegetation changes of the past 8 ka in North America (Shuman et al., 2005, 2009).

New evidence, however, challenges the hypothesis that the period of low hemlock abundance resulted from biotic interactions independent of climate. Evidence for regional to hemispheric climate change at ca 5.5 ka now includes reduced lake levels and other evidence of drought from Ontario to New Hampshire (Yu et al., 1997; Haas and McAndrews, 1999; Lavoie and Richard, 2000; Newby et al., 2000, 2009, 2011; Shuman et al., 2001, 2004, 2005, 2009; Muller et al., 2003; Booth et al., 2012), changes in atmospheric circulation (Yu et al., 1997; Kirby et al., 2002), and shifts in sea-surface temperatures (SSTs) (deMenocal et al., 2000; Sachs, 2007). Pollen records from areas near the range limits of hemlock also indicate climate change (Calcote, 2003; Foster et al., 2006), and importantly, show that hemlock did not change independently of other taxa.

The hemlock decline was concurrent with increases in *Fagus* (beech) and *Pinus* (pine) and decreases in *Quercus* (oak) populations in coastal Massachusetts (Tzedakis, 1992; Foster et al., 2006), as well as potentially synchronous (within dating uncertainties) beech declines (Williams, 1974; Shane and Anderson, 1993), *Ulmus* (elm) declines (Williams et al., 2004; Nelson et al., 2006; Grimm et al., 2009), and prairie expansion (Nelson et al., 2006) in the Midwest. However, the relative timing of the various climate and ecological changes has only been examined in detail at a few locations where simple cause-and-effect relationships were not apparent (Booth et al., 2012). The detailed site-specific analyses raise questions about the relative rates and timing of vegetation and moisture changes at local spatial scales and fine time scales (Booth et al., 2012), but the range-wide maintenance of low hemlock abundance and other contemporaneous features of the regional vegetation (e.g., high coastal beech abundance) for millennia after the decline could be consistent with the persistence of a new climatic regime, which also contributed to low lake levels and other changes (Shuman et al., 2004; Foster et al., 2006).

The role of temperature during these mid-Holocene changes has not been examined and may be essential to understanding the associated coastal oak-beech dynamics, in particular. In fact, pollen data from New England show different vegetation changes at inland and coastal sites (Foster et al., 2006), and suggest a persistent change in climate gradients across southern New England at the time of the hemlock decline. Decreases in oak and increases in beech populations might indicate that an increase in fog or other forms of effective moisture buffered the coast from drought experienced inland (e.g., Yu et al., 1997; Newby et al., 2011; Booth et al., 2012). Alternatively, the temperature gradient between coastal and inland sites across southern New England may have changed; a decrease in temperatures at the coast and an increase in temperatures at inland sites (ca 5.5 ka BP) could be consistent with the observed changes. Similar shifts in moisture and temperature gradients have been observed historically in association with atmospheric and ocean circulation changes in the AD 1960s when both temperatures and precipitation in New England were below normal during the most severe historic drought (Namias, 1966).

Testing these hypotheses requires investigations of both inland and coastal effective moisture and temperature histories. Effective moisture, discussed here as the balance of precipitation (P) and evapotranspiration (E), can be reconstructed by evaluating lake sediments to locate the position of lake shorelines through time using ground-penetrating radar (GPR) and various sedimentary analyses (Pribyl and Shuman, in review; Digerfeldt, 1986; Dearing, 1997; Shuman, 2003, 2005). For this study, we provide the record of lake-level changes at Deep Pond, a kettle lake located on Cape Cod, MA (Table 1, Fig. 1A) where the mid-Holocene oak decline and beech rise were first documented (Foster et al., 2006), and compare the lake-level record with effective moisture ($P-E$) data from inland sites to address the hypothesis that varying moisture levels during the mid-Holocene contributed to or sustained the hemlock decline.

We use regional sea-surface temperature (SST) reconstructions (Sachs, 2007) to help evaluate possible coastal temperature trends, but calibrate the pollen data themselves to quantify what temperature changes (if any) would be consistent with the abrupt vegetation changes. By doing so, we build on previous efforts to use pollen data to reconstruct regional climate gradients (Webb et al., 1993), but simply use the modern analog technique (MAT) (Overpeck et al., 1985; Guiot et al., 1993) to evaluate how the temperature and precipitation preferences of the regional vegetation changed. Because inferring a climatic cause of the vegetation changes from the pollen data would be circular, we use the approach to ask what magnitudes and directions of climate change could be consistent with the pollen record. Comparisons with the lake-level and SST records then enable us to evaluate whether the vegetation changes are consistent with the independently constrained climatic history.

We will evaluate three aspects of environmental change at the time of the hemlock decline: 1) past hydroclimatic trends at Deep Pond for comparison with inland water-level declines; 2) past changes in the temperature preferences of the coastal and inland vegetation; and 3) past agreement among vegetation climate preferences and independent climate indicators. We use our sediment-based lake-level reconstruction approach to pursue the hydroclimate changes, and then apply the MAT to pollen data to

Table 1
Sites in southern New England used in paleoenvironmental reconstructions.

Site	N latitude (degrees)	W longitude (degrees)	Elevation (m)	Number of ^{14}C dates	Number of pollen samples since 11 ka	Deep P-E vs. Precipitation preference correlation	Reference
Coastal						*0.90*	
Deep Pond	41.564	−70.635	23	14	140	0.88	Foster et al. (2006)
Duck Pond	41.933	−70.001	3	6	34	−0.04	Winkler (1985)
Fresh Pond	41.161	−71.579	28	5	35	0.84	Dunwiddie (1990)
No Bottom Pond	41.285	−70.114	8	4	35	0.67	Dunwiddie (1990)
Rogers Lake	41.367	−72.117	91	31	60	0.71	Davis (1969)
Inland						*0.80*	
Berry Pond West	42.505	−73.319	631	8	37	0.67	Whitehead (1979)
Blood Pond	42.08	−71.962	214	15	120	0.68	Oswald et al. (2007)
Little Pond – Royalston (LPR)	42.675	−72.192	302	7	80	0.72	Oswald et al. (2007)
Mohawk Pond	41.817	−73.283	360	12	34	0.72	Gaudreau (1986)
North Pond	42.651	−73.054	586	8	50	0.80	Whitehead and Crisman (1978)
Winneconnet Pond	41.971	−71.133	22	12	54	0.78	Suter (1985)

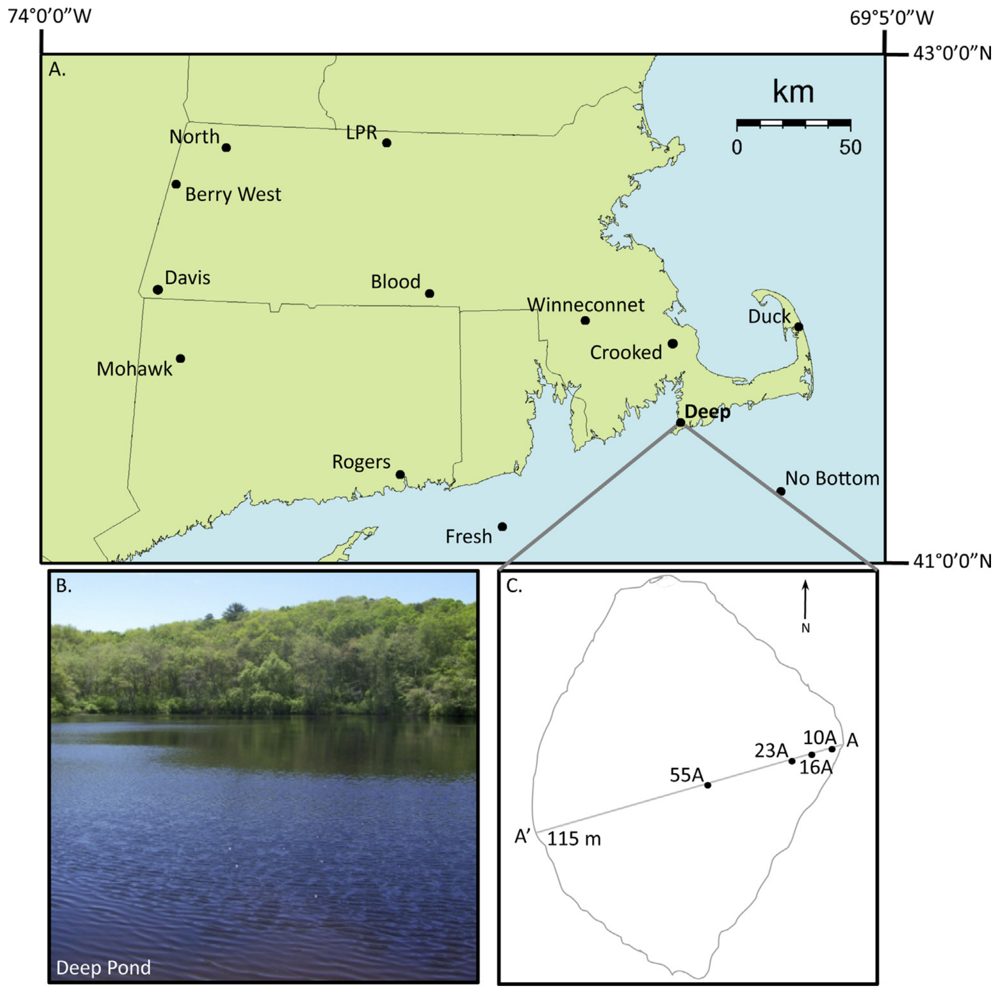

Fig. 1. A) Lake-level records and pollen study sites. B) Photo of Deep Pond showing the oak-deciduous forest surrounding the closed-basin kettle lake. C) Map of Deep Pond showing the GPR transect and core locations.

reconstruct the gradients and consistency of the vegetation climate preferences. We first apply the MAT to well-dated, detailed pollen data from a pair of inland and coastal sites in Massachusetts, Little Pond-Royalston (LPR) and Deep Pond, respectively (Table 1, Fig. 1A), and then use a wide array of available data (e.g., SST, lake level, and temperature preference data) from southern New England to examine the spatial patterns and potential drivers of mid-Holocene climate changes during the hemlock decline.

2. Methods

2.1. Lake-level and effective moisture reconstruction methods

2.1.1. Primary study site

We reconstruct the lake-level history of Deep Pond (41.581°N, −71.640°W, 23 m above sea level), a 0.89 ha, ~3.5-m-deep, closed-basin kettle lake at the base of Cape Cod near Falmouth, MA on the Buzzards Bay Moraine (Fig. 1). The pond lies within glacial till and outwash on a perched aquifer underlain by fine-grained sediments. The fine sediments isolate the pond from interactions with deep groundwater and sea-level fluctuations (Oldale, 1992), and allow lake-level fluctuations to result primarily from the climatically-controlled hydrologic budget of the ~8.47 ha (84,677 m^2) watershed. Results are compared to other lake-level reconstructions in Massachusetts: Crooked Pond (Shuman et al., 2001), New Long Pond (Newby et al., 2009; Shuman et al., 2009) and Davis Pond (Newby et al., 2011).

2.1.2. Field methods

To examine the water-level history of Deep Pond, geophysical surveys and sediment cores were collected along a 115-m east-west transect across the pond, and analyzed to evaluate past positions of the lake's shoreline (c.f. Digerfeldt, 1986; Shuman et al., 2001, 2005). Ancient shoreline positions were inferred from near-shore sand layers and associated sedimentary hiatuses generated when low lake levels prevented sediment accumulation in shallow areas of the basin (Digerfeldt, 1986; Dearing, 1997; Shuman, 2003; Shuman et al., 2001, 2005, 2009). A Geophysical Survey Systems, Inc. (GSSI) SIR-3000 GPR with a 200-MHz antenna was used to map the sediment geometry within Deep Pond and identify major sedimentary units that might be consistent with lake-level fluctuations. Changes in the amplitude of GPR returns indicate variations in the physical and chemical properties of the sediment (Moorman, 2001; Baker et al., 2007), and guided sediment core collection (Figs. 1C and 2A).

Six cores were collected in July 2009 along the shore-to-center transect using a modified square-rod piston corer (Wright, 1967), and complement an existing core from the center of the lake (Foster et al., 2006; core data described here); cores were labeled here by

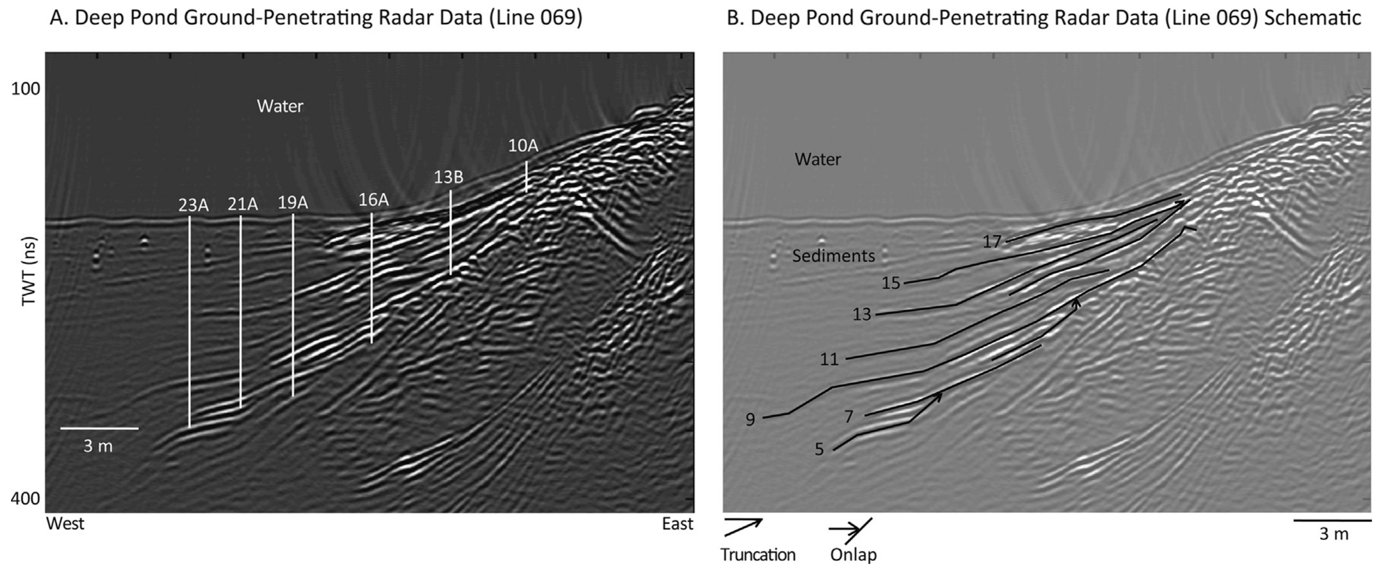

Fig. 2. A) Ground-penetrating radar profile moving from the center of the basin (left) towards the east shore (right) with two-way travel time (TWT) in nanoseconds along the *y*-axis and approximate position of core locations. B) Sedimentary features, such as onlaps and truncations, mapped onto the GPR profile. Numbers represent lowstands mentioned in the lake-level results.

distance from the eastern shore (e.g., 16A was retrieved 16 m west of the eastern shore; see Fig. 1C). Water depths for the six core locations (10A, 13B, 16A, 19A, 21A, and 23A) were 2.85, 3.29, 3.40, 3.46, 3.46, and 3.50-m, respectively.

2.1.3. Lab analyses

Once cores were collected, analyses of sediment lithology were conducted using high-resolution imagery, sediment density measurements, and loss-on-ignition (LOI) analysis. LOI at 550 °C was conducted using methods from Heiri et al. (2001) at contiguous 1-cm intervals throughout all cores to quantify changes in sediment composition. The LOI data were used to quantitatively constrain the past positions of littoral and deep-water sediments, and thus provide the basis for estimating changes in lake levels during the Holocene (see Fig. 3 and Appendix I for details). LOI analyses were supplemented by washing contiguous sediment samples through a 63 μm sieve, and applying the LOI procedure (Heiri et al., 2001) to the coarse fraction, to determine the sand content of selected cores.

The boundary between the deep-water (high LOI, low sand content) and littoral (low LOI, high sand) sediments is referred to as the ‘sediment limit’ (Digerfeldt, 1986), which forms where the mixed layer of the water column interacts with the lake bottom, re-mobilizing organic silts, and leaving behind sand and other inorganic materials. Based on core tops and surface samples from lakes in New England, modern deep-water sediments have greater than 75% LOI; littoral sediments (which are primarily sandy deposits) have less than 35% LOI. Transitional (sub-littoral) sediments have between 35 and 75% LOI, indicating a mix of organic-rich and sandy deposits.

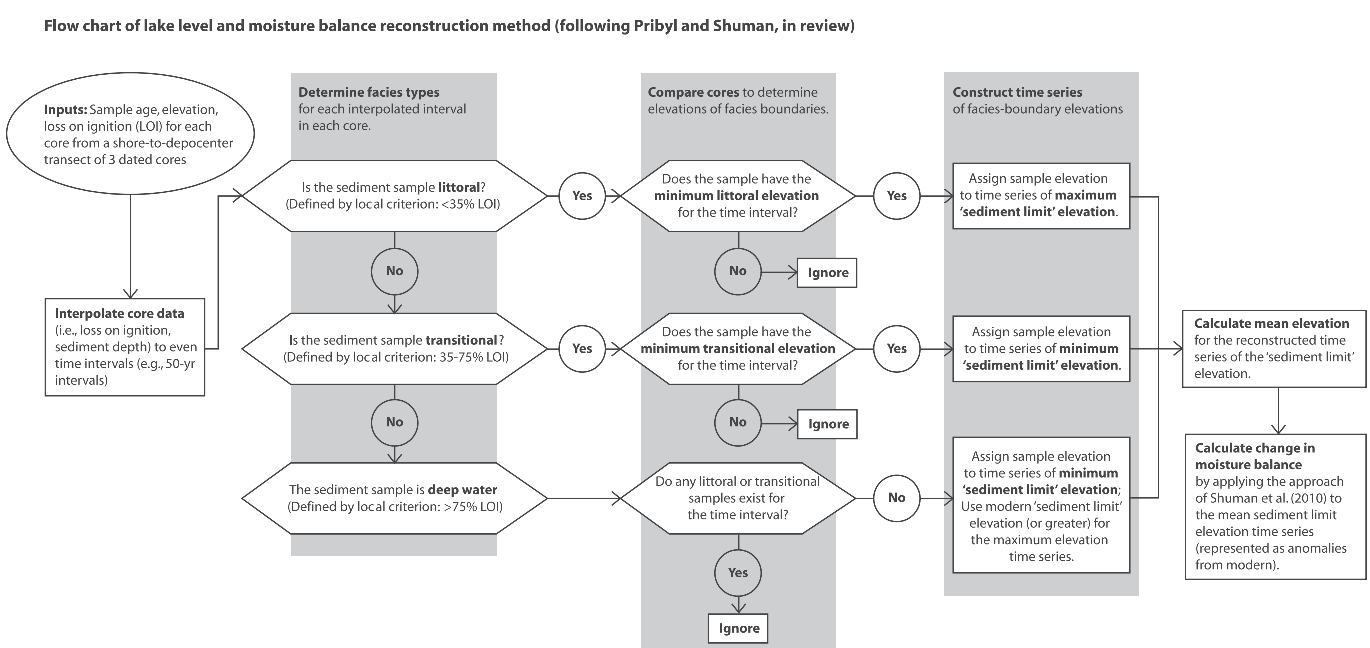

Fig. 3. Flow chart showing decision-tree approach to quantitatively reconstructing lake levels.

Table 2
Radiocarbon ages from Deep Pond cores.

No.	Core	Depth below modern lake surface	NOSAMS/Keck lab no.	^{14}C yr BP	Age error 1-Sigma	Bchron 50% (Cal yr BP)	Bchron 2.5% (Cal yr BP)	Bchron 97.5% (Cal yr BP)	Material dated	Type 1 or 2 outliers
1	10A	303.5	OS-80696	340	25	389	317	481	Bulk sediment	
2	10A	303.5	UCIAMS# 73606	680	20	657	568	672	Charcoal	
3	10A	320.5	OS-80697	710	30	668	571	697	Bulk sediment	1
4	10A	320.5	UCIAMS# 73607	630	15	593	560	654	Charcoal	
5	10A	347	UCIAMS# 73608	1685	15	1582	1542	1681	Charcoal	
6	10A	347	OS-80698	1750	25	1655	1577	1720	Bulk sediment	
7	10A	360.5	UCIAMS# 73609	2135	20	2122	2030	2287	Charcoal	
8	10A	360.5	OS-80699	2180	25	2246	2122	2303	Bulk sediment	
9	10A	365.5	UCIAMS# 78233	2290	15	2334	2212	2345	Charcoal	
10	10A	377.5	UCIAMS# 78234	2190	15	2252	2149	2302	Charcoal	
11	10A	402.5	UCIAMS# 78235	2980	15	3170	3083	3237	Charcoal	
12	16A	441.5	UCIAMS# 78232	1215	15	1137	1074	1223	Charcoal	
13	16A	450.5	UCIAMS# 78231	1470	15	1354	1315	1388	Charcoal	
14	16A	523.5	UCIAMS# 73610	3385	15	3631	3581	3685	Charcoal	
15	16A	523.5	OS-80700	3440	30	3697	3617	3819	Bulk sediment	
16	16A	543.5	OS- 80703	3940	30	4390	4270	4504	Bulk sediment	
17	16A	562.5	OS-80701	4430	40	5024	4882	5268	Bulk sediment	
18	16A	562.5	UCIAMS# 73611	4450	30	5105	4918	5271	Charcoal	
19	16A	573.5	UCIAMS# 73612	4965	15	5689	5651	5728	Charcoal	
20	16A	573.5	OS-80702	4710	30	5417	5329	5573	Bulk sediment	
21	16A	578.5	UCIAMS# 78230	6220	20	7114	7025	7237	Charcoal	2
22	16A	606.5	UCIAMS# 78229	6975	15	7811	7745	7908	Charcoal	
23	23A	429.5	OS-87471	455	30	510	472	533	Bulk sediment	
24	23A	473.5	OS-87472	1040	30	951	922	1044	Bulk sediment	
25	23A	503	UCIAMS# 90202	1940	20	1888	1831	1937	Charcoal	
26	23A	558	UCIAMS# 90203	1670	20	1566	1531	1680	Charcoal	2
27	23A	614.5	UCIAMS# 90204	3000	20	3200	3087	3310	Charcoal	
28	23A	625.5	OS-87473	3420	25	3668	3595	3806	Bulk sediment	
29	23A	658	UCIAMS# 90205	3975	20	4449	4416	4513	Charcoal	
30	23A	682.5	OS-87474	4430	30	5014	4887	5260	Bulk sediment	
31	23A	706.5	OS-87475	4910	50	5641	5567	5749	Bulk sediment	
32	23A	718.5	UCIAMS# 90206	5250	20	5987	5938	6167	Charcoal	2
33	23A	733.5	UCIAMS# 90207	5025	20	5829	5676	5883	Charcoal	
34	23A	745.5	UCIAMS# 90208	5350	25	6133	6013	6261	Charcoal	
35	23A	779.5	OS-87476	5490	30	6291	6219	6382	Bulk sediment	
36	23A	816.5	UCIAMS# 90209	5520	25	6308	6285	6391	Charcoal	
37	55A	406	N/A	N/A	N/A	85	N/A	N/A	^{210}Pb dating	
38	55A	452	N/A	N/A	N/A	290	N/A	N/A	Euro. settlement	
39	55A	463	AA 37215	670	60	628	548	710	Bulk sediment	
40	55A	478	AA 35298	700	40	660	565	710	Bulk sediment	
41	55A	498	AA 35299	1090	40	1000	935	1104	Bulk sediment	
42	55A	537	AA 37216	1780	40	1702	1582	1814	Bulk sediment	
43	55A	603	AA 35300	2310	50	2325	2166	2470	Bulk sediment	
44	55A	675	AA 57240	2900	30	3035	2950	3156	Bulk sediment	
45	55A	768.5	OS-102255	3820	20	4198	4148	4290	Bulk sediment	1
46	55A	843	AA 57241	4420	40	5007	4878	5263	Bulk sediment	
47	55A	855.5	UCIAMS# 115863	4830	80	5552	5340	5729	Charcoal	
48	55A	867.5	UCIAMS# 115862	4700	15	5373	5329	5567	Charcoal	
49	55A	968.5	OS-102254	5910	40	6730	6656	6843	Bulk sediment	
50	55A	1068	AA 57242	7360	50	8176	8039	8316	Bulk sediment	
51	55A	1143	AA 57243	8810	50	9852	9655	10,135	Bulk sediment	
52	55A	1168	AA 57244	10,080	50	11648	11,378	11,941	Bulk sediment	
53	55A	1188	AA 57245	12,840	60	15303	14,994	15,912	Bulk sediment	

Near-shore sand layers are interpreted as periods of low water when the elevation of the sediment limit declined, as long as the radiocarbon dates (Table 2) confirm slowed sedimentation rates, rather than instantaneous deposits (e.g., a slump or flood). By correlating the dates and elevations of sand layers across multiple cores, the timing and magnitude of droughts can be constrained. Four of the cores have been radiocarbon dated and are used in this study to quantitatively reconstruct the lake-level and effective moisture history at Deep Pond (Fig. 3; Appendix I).

2.1.4. Deep Pond chronology

Accelerated mass spectroscopy (AMS) ^{14}C analysis of bulk sediment and macroscopic charcoal constrain the chronologies of cores 10A, 16A, 23A and 55A. Additionally, the ages of the uppermost sediment from 55A are constrained by ^{210}Pb and the age of the *Ambrosia* rise determined from a rise in *Ambrosia* pollen (Table 2). The ^{14}C dates were calibrated using the INTCAL09 terrestrial calibration curve (Reimer et al., 2009); we used a Bayesian age-modeling approach (Bchron) to calculate uncertainty between dated points in each core (Parnell et al., 2008). Because Bchron only assumes that a given unit of sediment must be younger than the sediments below it, the approach to fitting ages to samples between radiocarbon dates performs well in littoral cores with rapid sedimentation rate changes. Bchron also contains an algorithm for determining outlier radiocarbon dates, which can be a concern where erosion during low-water leads to re-deposition of old material. Bchron places outliers into two categories: 1) Type 1 outliers that only require a small age shift to assure monotonicity in the age–depth relationships determined by other ages, and 2) Type 2 outliers that are difficult to reconcile

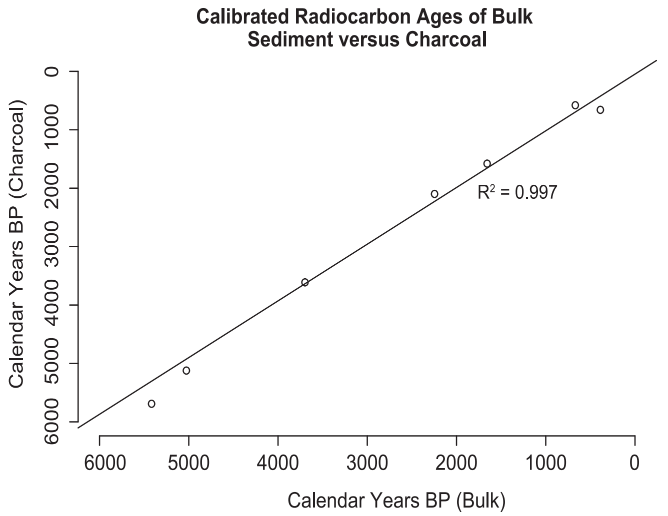

Fig. 4. Scatter plot showing the correlation between the calibrated radiocarbon ages of charcoal and bulk sediment from the same intervals in cores 10A and 16A ($n = 7$).

with the other possible age–depth relationships. Type 2 outliers are discarded here, and the remaining dates used in Bchron to produce the final core chronology (Parnell et al., 2008; see Table 2 for outliers and types).

Charcoal and bulk radiocarbon dates were also directly compared at seven intervals in cores 10A and 16A to determine if 'old carbon' affected the bulk sediment dates (Fig. 4; Grimm et al., 2009; Oswald et al., 2005). Charcoal or other macrofossil material was not available to date at all major stratigraphic positions, and bulk sediment was dated instead. Because Bchron allows only one radiocarbon date to be used per depth interval, we averaged the two dates at the seven intervals in 10A and 16A before running Bchron to produce the final core chronologies (Fig. 5).

2.2. Pollen-based climate reconstructions

2.2.1. Modern and fossil pollen datasets

We quantify the apparent climatic preferences of the past vegetation at Deep Pond and other southern New England sites by matching the fossil pollen data to potential analogs in a network of 4,549 surface pollen samples with associated modern climate data from across northeastern and boreal North America (i.e., a subset of the North American modern pollen data compiled by Whitmore et al., 2005, excluding the western and southeastern U.S.). Counts exist for 134 pollen types, but for this study we focus on 58 pollen types found in the northeastern United States (consistent with recommendations by Williams and Shuman, 2008) (Table 3).

Fossil pollen data spanning 12 ka to present were chosen from five coastal sites and six inland sites (Table 1, Fig. 1A). The sites span 41°–43° north latitude and 70°–73° west longitude, and were chosen for their high temporal resolution, as well as their full spatial coverage of the region of interest.

All sites have radiocarbon chronologies that were calibrated to years before AD 1950 for previous work (Williams et al., 2004; Foster et al., 2006; Oswald et al., 2007). Based on the existing chronologies, the pollen data were linearly interpolated to 100-year time steps to facilitate inter-site comparison of the pollen-inferred paleoclimate reconstructions.

2.2.2. Modern analog technique (MAT)

We use the MAT to reconstruct the climatic preferences of the past vegetation from fossil pollen assemblages (Overpeck et al., 1985). Our approach compared each fossil pollen assemblage to all assemblages from the modern pollen dataset using the squared chord distance (SCD) metric (Overpeck et al., 1985). The climatic conditions associated with seven 'best modern analogs' (i.e., with the lowest SCDs) were then averaged to assign modern climatic variables to each fossil assemblage as suggested by Williams and Shuman (2008).

Reconstruction quality was established using a 'leave-one-out' cross-validation study that used modern pollen assemblages to reconstruct modern climatic variables (Table 4). Telford and Birks

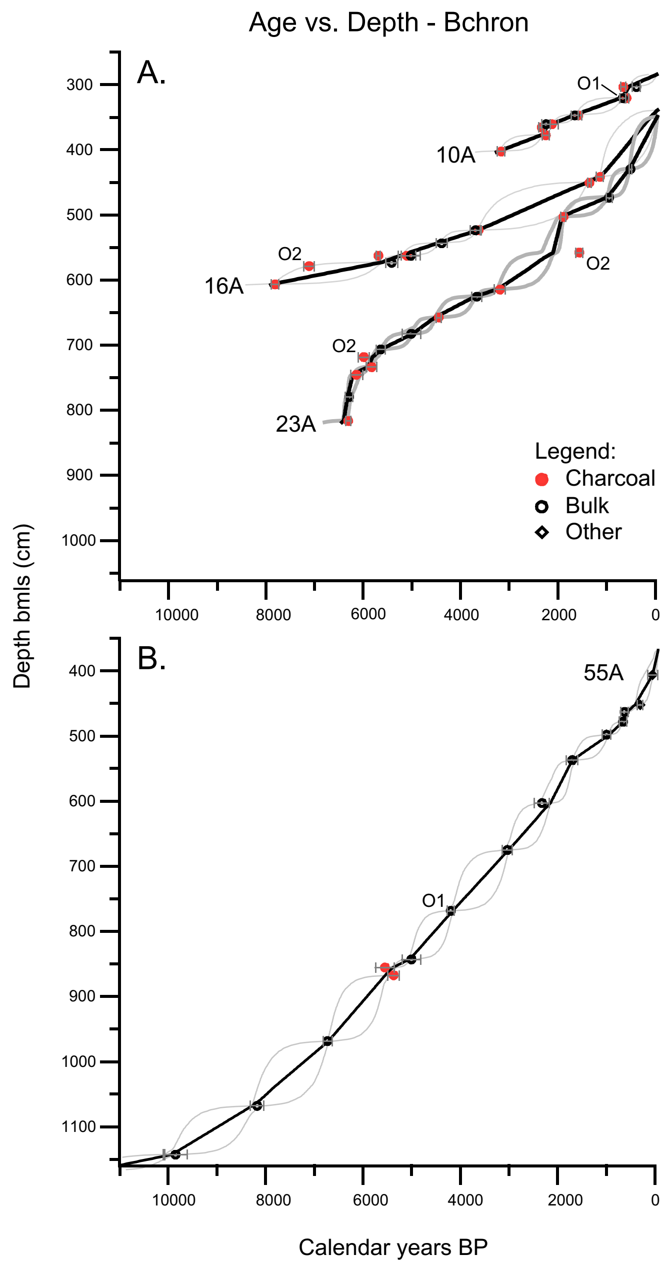

Fig. 5. A) Bchron age–depth plots with calibrated ages and uncertainties from cores 10A, 16A, and 23A. Depth below modern lake surface is along the y-axis, with calibrated ages before 1950 AD along the x-axis. Black lines indicate the mean calibrated chronology, with gray bands indicating the 95% age distribution between dates. B) Same as A, but for core 55A. Charcoal dates are indicated as red circles, bulk sediment dates as open circles, and ages assigned based on ^{210}Pb and pollen stratigraphic analyses as open diamonds. O1 = Type 1 outlier, O2 = Type 2 outlier. (For interpretation of the references to color in this figure legend, the reader is referred to the web version of this article.)

Table 3
Taxa used in modern analog technique reconstructions.

Scientific name	Common Name
Abies	Fir
ACER[a]	Maple
ALNUS[b]	Alder
Aquifoliaceae	Holly Family
Arceuthobium	Mistletoe
Artemisia	Sagebrush, wormwood
ASTERACEAE[c]	Daisy Family
Betula	Birch
Brassicaceae	Mustard Family
Cactaceae	Cactus Family
Carya	Hickory
Caryophyllaceae	Chickweed Family
Castanea	Chestnut
Celtis	Hackberry
Cephalanthus	Buttonbush
Chenopodiaceae/Amaranthaceae	Goosefoot/Pigweed Families
Chrysolepis/Lithocarpus	Chinquapin/Tanoak
Corylus	Hazel
Cupressaceae	Cedar Family
Cyperaceae	Sedge Family
Dryas	Mountain Avens
Ephedra	Jointfir
ERICACEAE[d]	Heath Family
Fagus	Beech
Fraxinus nigra	Black Ash
Fraxinus pennsylvanica/americana	White/Green Ash
Fraxinus undifferentiated	Ash undiff.
JUGLANS[e]	Walnut
Larix/Pseudotsuga	Larch/Douglas Fir
Larrea	Creosote Bush
Liquidambar	Sweetgum
LYCOPODIUM[f]	Club moss
MINOR FORBS[g]	Minor Forbs
Myricaceae	Myrtle Family
Nyssa	Sourgum
Ostrya/Carpinus	Hophornbeam, Hornbeam
Oxyria	Mountain Sorrel
Papaveraceae	Poppy Family
PICEA[h]	Spruce
Pinus diploxylon	Hard Pines
Pinus haploxylon	Soft Pines
Pinus undifferentiated	Pine undiff.
Plantaginaceae	Plantain Family
Platanus	Sycamore
Poaceae	Grass Family
Populus	Poplar, Aspen
Prosopis	Mesquite
Pteridium	Bracken (fern)
Quercus	Oak
Rosaceae	Rose Family
Salix	Willow
Sarcobatus	Greasewood
SAXIFRAGA[i]	Saxifrage
Sphagnum	Peat moss
Taxodium	Cypress
Tilia	Basswood
Tsuga[j]	Hemlock
Ulmus	Elm

[a] Sum of *Acer negundo, A. rubrum, A. saccharum, A. undiff.*
[b] Sum of *Alnus rugosa, A. undiff.*
[c] Sum of *Iva.*
[d] Sum of *Ericaceae undiff.*
[e] Sum of *Juglans cinerea, J. nigra, J. undiff.*
[f] Sum of *Lycopodium annotinum, L. clavatum, L. inundatum, L. lucidulum, L. selago, L. undiff.*
[g] Sum of Apiaceae.
[h] Sum of *Picea glauca, P. mariana, P. undiff.*
[i] Sum of *Saxifraga oppositifolia.*
[j] Sum of *Tsuga heterophylla, T. mertensiana, T. undiff.*

Table 4
Root mean squared error and R^2 values from leave-one-out cross-validation test.

Climatic variables	RMSE	R^2
July Temperature (°C)	1.26	0.94
Annual Precipitation (mm)	165.99	0.70

(2005) point out that R^2 values overestimate the predictive power of paleoclimate reconstructions using the MAT because of spatial autocorrelation in the response variables. However, this issue is common to all cross-validation analyses (Williams and Shuman, 2008; Bartlein et al., 2010), and thus R^2 values are used here as a relative metric of skill among variables and decisions associated with using the MAT.

3. Results

3.1. Lake-level changes at Deep Pond

Stratigraphic changes at Deep Pond show evidence of a long-term rise in water levels based on shoreward expansion of deep-water sediments (Figs. 6 and 7). The rise culminated in high water after ca 3 ka consistent with other regional reconstructions (e.g., Shuman et al., 2001). Additionally, 17 stratigraphic units, including 8 high LOI units (even numbered events) and 9 low LOI units (odd numbered events), interrupt the long-term shoreward expansion of sediments (Figs. 6 and 7). The low LOI units correlate with a series of bright reflectors in the GPR profile (Fig. 2B). Similar units are also observed at other Massachusetts lakes, such as New Long and Davis Ponds (Newby et al., 2009, 2011).

We interpret the stratigraphic units below. All depths discussed are relative to the modern lake surface. The ages of the units derive from AMS radiocarbon ages of both charcoal and bulk sediment because bulk sediment ages appear to have no meaningful difference from charcoal ages obtained from the same intervals ($R^2 = 0.997$; Fig. 4). In fact, charcoal rather than bulk sediment ages appear too old at some intervals where both bulk sediment and charcoal ages were obtained, possibly due to landscape storage or sediment re-working associated with erosion during low water. Similarly, the Bchron chronologies for all four dated cores (Table 2, Fig. 5) reveal a few outlier ages.

3.1.1. Evidence of a Holocene-scale water-level rise

Based on the central core, 55A, Deep Pond formed by ca 15.1 ka (Table 2). Both GPR and near-shore cores indicate, however, that the early stratigraphic units (1–7) accumulated in the center of the basin before 8 ka and are only captured in 55A (Figs. 6 and 7). Therefore, units 1–7 are not discussed at length here.

After 8 ka, LOI in 55A rises and remains above 60%, which is consistent with a rise in the water surface and uninterrupted organic sediment accumulation in the center of the basin for the remainder of the Holocene. Cores near to shore then constrain the lake-level history.

The basal ages from core 16A of 7.8 ka and core 23A of 6.4 ka indicate that lake levels had risen enough by the mid-Holocene to allow littoral and transitional sediments to start accumulating at intermediate depths in the basin (Figs. 6 and 7). However, sands dominate 23A below 743 cm depth (ca 6.1 ka) and 16A below 580 cm depth (ca 6.0 ka). We interpret the deposition of organic silts above the sands (highstand unit 8) to represent a further rise in lake level. Layers of low LOI sand above 702 cm depth in core 23A and above 559 cm depth in 16A mark the end of the water-level rise. These layers, and others above them,

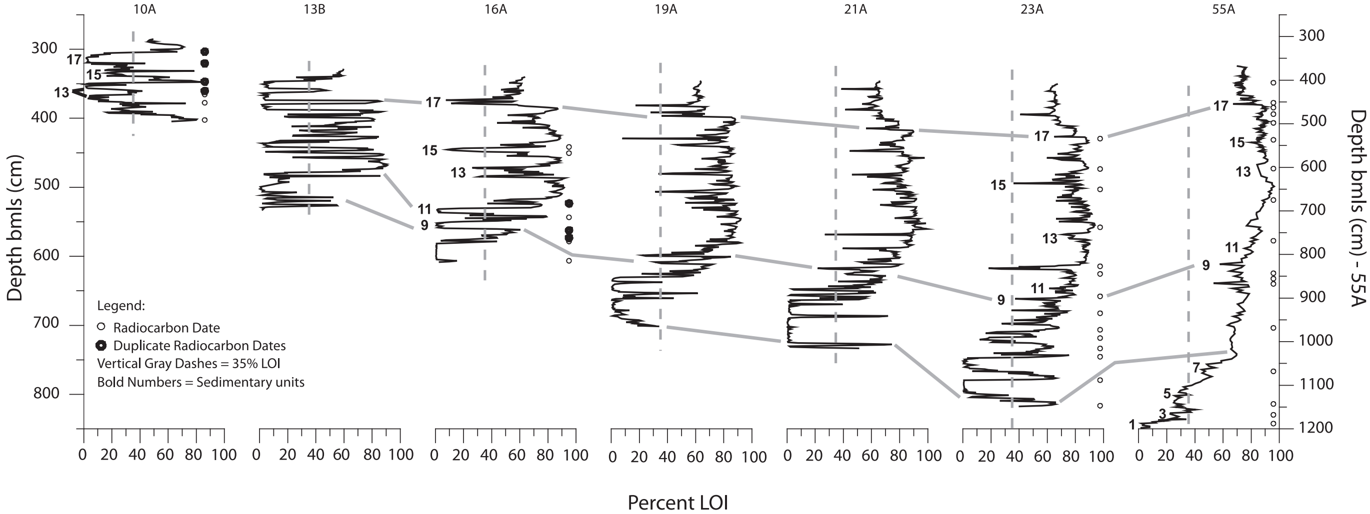

Fig. 6. Loss-on-ignition data for all cores in the transect plotted as depth below the modern lake surface (bmls). Open circles represent depths of radiocarbon ages. Gray lines track major stratigraphic boundaries, and low LOI intervals associated with lowstands are labeled by the unit numbers mentioned in the text (e.g., 13, 15, 17, etc.).

become thinner and less pronounced in deeper cores (Fig. 6), consistent with near-shore sand accumulation during periods of low water (units 9–17).

Core 10A has a basal age of 3.6 ka (Figs. 6 and 7), indicating that the highest lake levels were only reached in the late-Holocene when transitional sediments began to accumulate in the shallowest part of the basin (starting with highstand unit 12; Fig. 6). Like core 16A, 10A contains an alternating series of sand (low LOI) and silt (high LOI) layers consistent with additional fluctuations (units 13–17), which punctuated the long-term rise in water level and are discussed further below.

3.1.2. Evidence for low-water episodes associated with the hemlock decline

Multi-century variability in lake levels between 6.1 and 3.9 ka produced a series of stratigraphic changes including abrupt shifts

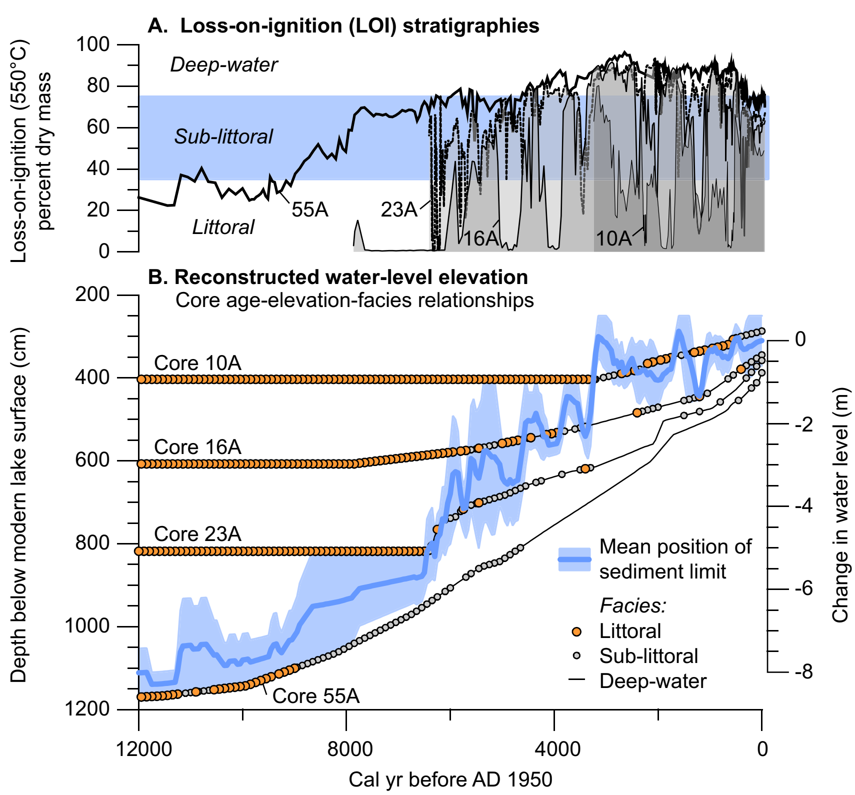

Fig. 7. A) Loss-on-ignition (LOI) data for cores 55A (solid line), 23A (dashed line), 16A (light gray shading), and 10A (dark gray shading) plotted versus time and relative to littoral, sub-littoral, and deep-water facies thresholds (horizontal blue bar) representative of the 18 iterations applied (see Appendix I). B) Age–depth relationships for the four cores plotted with facies types shown based on the LOI thresholds used above. Yellow circles indicate littoral sediments, gray circles represent sub-littoral sediments, and the black line denotes deep-water sediments. These data provide the constraints for the reconstructed position of the 'sediment limit' through time, which is shown as a blue line with a light blue band indicating the range of uncertainty in its position determined by applying 18 different sets of facies thresholds (see Appendix I). (For interpretation of the references to color in this figure legend, the reader is referred to the web version of this article.)

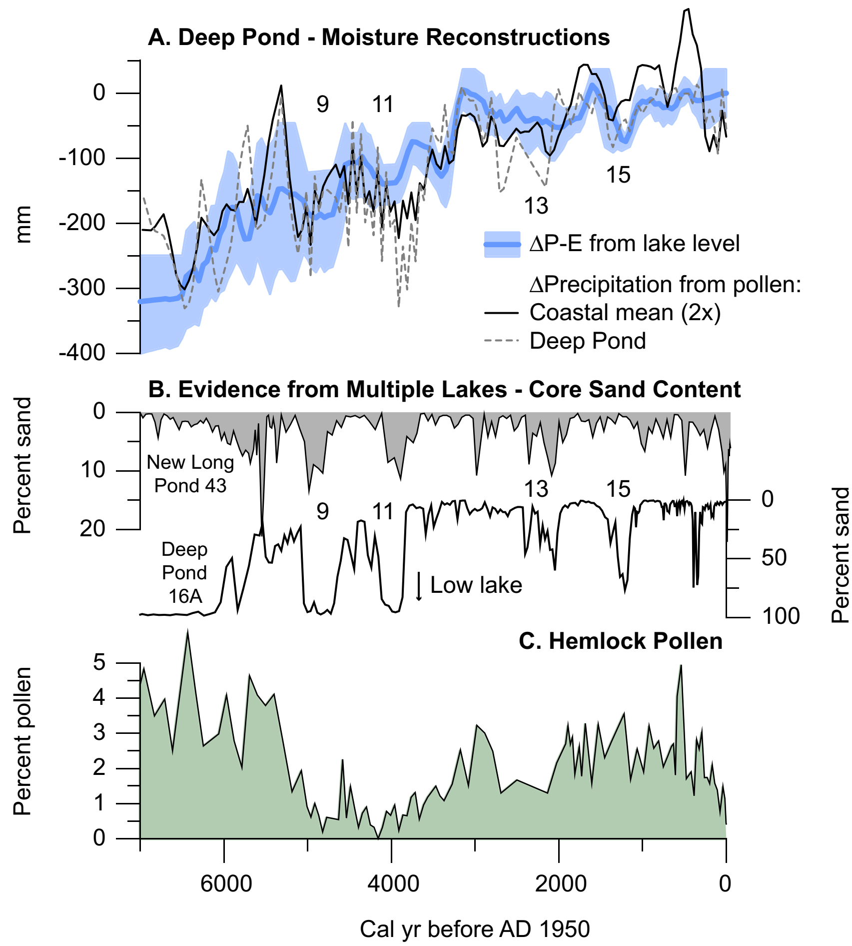

Fig. 8. A) Deep Pond moisture reconstruction (ΔP–E) based on the sedimentary data (solid blue line with light blue uncertainty; derived from Fig. 7B and iterative moisture-budget calculations) plotted with pollen-inferred changes in the precipitation preference of the vegetation at Deep Pond (dashed line) and the average of all coastal sites (×2; black line). The pollen-inferred values (interpolated to 100-yr intervals) are plotted relative to the reconstructed pre-settlement value at 500 calendar years before 1950 AD. B) Grain size data from New Long Pond, MA (Core 43; Shuman et al., 2009) and Deep Pond, MA (Core 16A). Large grain size values are interpreted as evidence for low water; note inverted scales. Numbers label lowstands consistent with those in the text. C) Deep Pond hemlock pollen percentages. (For interpretation of the references to color in this figure legend, the reader is referred to the web version of this article.)

from transitional silts to littoral sand (lowstand unit 9) in core 23A after 5.5 ka (702 cm depth; Figs. 6 and 7) and in core 16A after 5.1 ka (559 cm depth). The onset of the simultaneous hemlock and oak declines recorded by pollen in the center core (55A) also dates to 5.4 (5.5–5.3) ka (Fig. 8). The lowstand (unit 9) persisted until ca 4.6 ka when organic silt deposition above 546 cm depth in 16A marks highstand unit 10 and hemlock pollen percentages briefly increase in core 55A (Fig. 8). After only ∼200 years, however, the sediment type in 16A shifted back to sands during lowstand unit 11, and hemlock pollen percentages declined for a second time (Fig. 8). The base of the second sand layer in 16A (lowstand unit 11) at 541 cm depth dates to 4.3 ka (Figs. 6 and 7). Unit 11 appears in core 23A as a change from deep water to sub-littoral sediments at 652 cm depth at ca 4.4 ka.

3.1.3. *Late-Holocene fluctuations – 3.8 ka to present*

Lake levels rose after lowstand 11 and were high (unit 12) from ca 3.9–3.0 ka, based on the accumulation of organic silts at 640 cm depth in 23A, at 530 cm depth in 16A and at 404 cm depth in core 10A. Unit 12 also appears as an interval of high organic silt near the base of core 13B (Fig. 6). A peak in hemlock pollen percentages coincides in time with the unit 12 highstand (Fig. 8).

A decline in LOI and renewed sand accumulation in 10A at ca 2.9 ka and in 16A by ca 2.4 ka (484 cm depth) marks lowstand unit 13 (Figs. 6 and 7). The sands signal a potentially time-transgressive decline in water levels spanning ∼0.5 ka as measured across these two cores. The subsequent low levels persist until after 2.3 ka when sediments in core 16A shift back to transitional silts at 481 cm depth. A similar change followed in 10A at ca 1.9 ka (at 348 cm depth).

The organic silts in 16A above 481 cm and in 10A above 348 cm depth mark highstand unit 14, but were immediately overlain by littoral sands (lowstand unit 15) at ca 1.3 ka in both 16A and 10A (at 448 cm and 330 cm depths, respectively). Above unit 15, deep-water silts accumulated in core 16A and indicate high water beginning at ca 1.05 ka, which have continued until present except briefly at ca 0.6 ka (lowstand 17). Lowstand 17 also appears as littoral sands in 10A (0.6–0.4 ka; Figs. 6 and 7).

3.2. *Deep Pond quantitative lake level and moisture balance reconstruction*

The changing elevations of the sediment limit at Deep Pond (Fig. 7) indicate that the water level likely rose by >800 cm since 12 ka. Based on systematic interpretation of the sedimentary data and calculation of the watershed moisture budget (Figs. 2 and 7), ΔP–E would have increased by 445 mm over the Holocene. The short-term events (recorded by units 9–17) superimpose changes of 50–150 mm on century to millennium scales on the long-term trend. For example, during lowstand unit 9 (5.5–4.6 ka), and the hemlock and oak declines at ca 5.4 ka, core elevations indicate that the sediment limit fell to ~400 cm lower than today (Fig. 7B), and that $\Delta P{-}E$ was ~200 mm lower than today (Fig. 8A, black line) because effective moisture decreased by ~50 mm relative to the baseline conditions at ca 5.5 ka (Fig. 8A). Earlier (>8 ka) millennial-scale changes in $\Delta P{-}E$ are, however, difficult to interpret because only one dated core (55A) constrains the position of the shoreline at Deep Pond (Table 2).

3.3. Comparison with pollen-inferred vegetation precipitation requirements

The annual precipitation requirements of the vegetation inferred from the pollen data from Deep Pond using the MAT (Fig. 8A, dashed line) closely correlate ($r = 0.88$) with the independently reconstructed $\Delta P{-}E$ changes constrained by the sediment record of lake-level change (Fig. 8A, black line). As with the lake-level reconstruction, pollen-inferred annual precipitation requirements at Deep Pond increased progressively throughout the Holocene (~475 mm over the last 11 ka, ~250 mm over the last 7 ka), and show millennial-scale variations that punctuate the long trend. The short-term changes in the vegetation moisture preferences often correspond to high and low water episodes in the independent lake-level reconstruction, and the correlation improves ($r = 0.90$) when data from multiple sites are averaged together (Fig. 8A; Table 1). A Granger causality test comparing the Deep Pond $\Delta P{-}E$ and precipitation-requirement reconstruction, and accounting for autocorrelation in the time-series, confirms significant correlations ($F = 12.61$; $p = 0.0004$), although the correlation based on the median sample ages decreases when the long-term, linear trends have been removed ($r = 0.17$ over the interval of the detailed lake-level history since 6 ka).

The changes in pollen-inferred precipitation requirements include a pair of episodes at 5.4–4.4 and 4.2–3.8 ka when the vegetation trended in a xeric direction consistent with lowstands 9 and 11, which are recorded by a pair of low-water sand layers at both Deep and New Long Ponds (Fig. 8B); New Long Pond is situated 50 km north in Plymouth near the coast of mainland Massachusetts, and >50 radiocarbon ages constrain its water-level history (Newby et al., 2009; Shuman et al., 2009). The xeric episodes include the two-phase period of low hemlock abundance at Deep Pond from 5.4 to 3.8 ka (Fig. 8C). A brief highstand of the ponds (unit 10) correlates with a mesic interval between the xeric episodes, and correlates with a brief recovery of hemlock pollen percentages (Fig. 8C).

Similarly, the annual precipitation requirements of the vegetation at a well-resolved, inland site, Little Pond-Royalston (LPR), also show a long-term increase (~800–1000 mm) with a superimposed series of multi-century variations between 900 and 1100 mm (Fig. 9C). The precipitation-requirement reconstructions from LPR

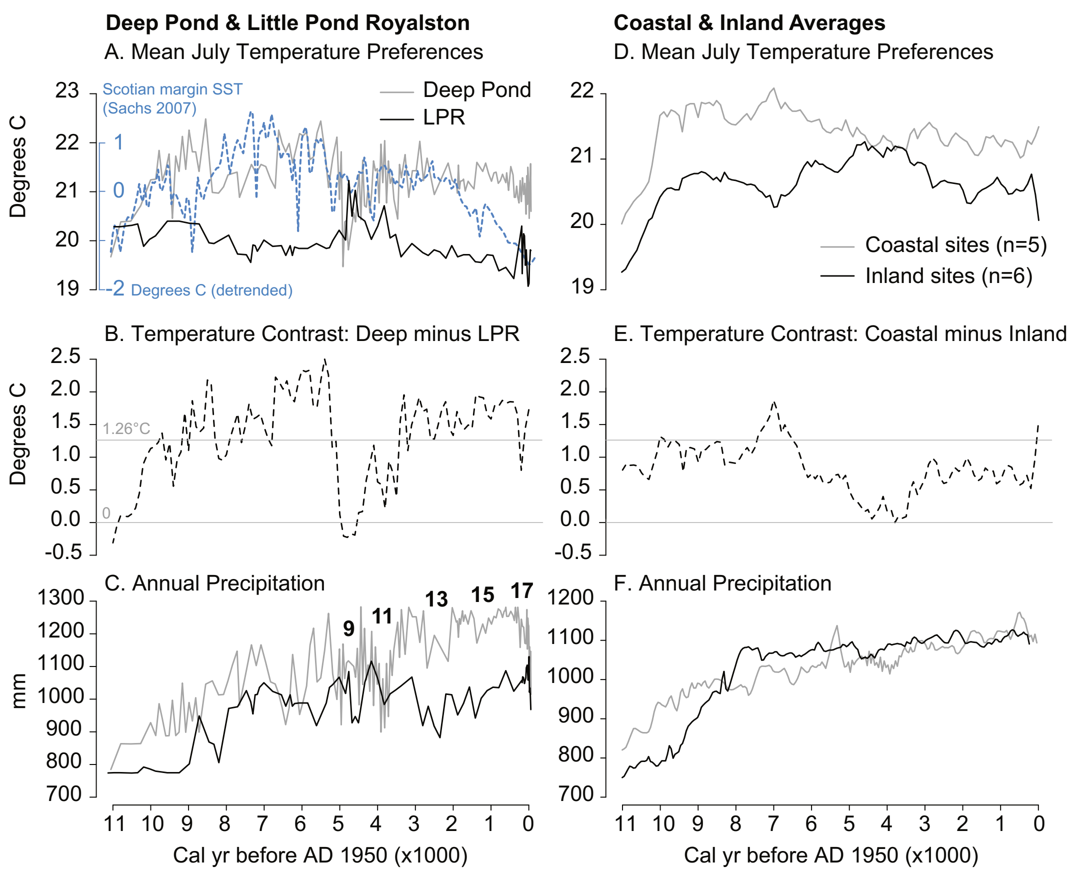

Fig. 9. A) Pollen-inferred July temperature preferences for Deep Pond (gray) and Little Pond-Royalston (LPR; black). Sea surface temperatures (SSTs) from alkenones off the coast of Nova Scotia are shown in blue (Sachs, 2007). B) July temperature preferences for Deep Pond minus LPR (dashed). C) Annual precipitation preferences for Deep Pond and LPR, with lowstands 9-17 labeled. D) Pollen-inferred July temperature preferences for the averages of coastal (gray) and inland (black) sites in southern New England. E) July temperature preferences for coastal sites minus inland sites (dashed). F) Annual precipitation preferences for coastal and inland sites. Horizontal gray lines in B and E indicate the range of positive temperature-preference differences that are not significantly different from zero. To emphasize abrupt changes and minimize artifacts associated with seasonality changes in alkenone data, a long-term trend has been removed from the SST reconstruction in A. Degrees Celsius appears along the y-axis for panels A, B, D and E, and millimeters of precipitation for panels C and F. Calendar years before 1950 AD along the x-axis.

and Deep Pond both appear to capture xeric shifts in the vegetation during lowstand events 9–17 (Fig. 9C). Even the two low $\Delta P-E$ episodes at Deep Pond that make up lowstand 13 (see the pair of low LOI intervals in core 10A and 16A at ca 2.9–2.4 ka; Figs. 7 and 8) appear in both pollen-based precipitation-requirement reconstructions (Figs. 8 and 9C).

Precipitation-requirement reconstructions from nine of the remaining ten sites across southern New England also correlate with the Deep Pond lake-level reconstruction with correlation coefficients of 0.67–0.88 (Table 1), excluding Duck Pond. The exception at Duck Pond ($r = -0.04$) on the outer portion of Cape Cod may confirm the potential influence of local ecological factors on the inferred precipitation requirements at individual sites because fires and sandy soils maintained oak-pine scrub through the Holocene despite various climate changes (Winkler, 1985).

3.4. Vegetation temperature preferences

Because drought recorded by low lake levels coincided with the abrupt vegetation changes (e.g., the hemlock decline) at ca 5.4 ka at both inland (Newby et al., 2011) and coastal sites, such as Deep Pond, moisture differences (e.g., coastal fog) do not appear to explain the differences in inland and coastal vegetation changes (e.g., opposite directions of oak, beech, and pine change associated with the hemlock decline). To investigate an alternative cause of the differences, we used the MAT to evaluate the regional temperature changes. If temperature were important, we expect to detect a difference in inland versus coastal temperature preferences at the time of the hemlock decline, and that any change in coastal preferences would be consistent with regional SST changes. To further avoid circularity in interpreting the results, we removed hemlock from the pollen sums, and found that the inclusion or removal of hemlock had a minimal effect on the temperature preference reconstructions. The results discussed below include hemlock to provide a complete assessment of the temperature-preference (vegetation-composition) changes.

3.4.1. Inland-coastal comparison

Mean July temperature preferences were first reconstructed from Deep Pond and Little Pond-Royalston using the detailed pollen data from each site (Fig. 9A, B). The reconstruction confirms that the vegetation at Deep Pond shifted in favor of cool-tolerant taxa (beech over oak) after ca 5.4 ka (Fig. 9A). At the same time, the mean July temperature reconstructed from the vegetation at LPR increased (Fig. 9A) because intermediate percentages of oak and pine pollen replaced high hemlock pollen percentages and caused the selection of warm modern analogs. By ca 3 ka, the pollen records from both sites indicate a return to near pre-5.4 ka temperature preferences. The difference in thermal preferences between LPR and Deep Pond could be consistent with an abrupt decline in the inland-coastal gradient of July temperatures by >2 °C at 5.4 ka; the difference shifted from exceeding the magnitude of uncertainty in the reconstructions (1.26 °C; Table 4) before 5.4 ka to near zero after (horizontal gray lines; Fig. 9B).

The broad network of pollen records indicates that the vegetation histories consistently record a rapid weakening of the inland-coastal gradient in temperature preferences at ca 5.4 ka (Fig. 9E). The contrast in thermal preferences remained lower than any time in the Holocene until ca 4 ka. The time series of the regional averages (Fig. 9D–F) are smoother than the individual site reconstructions (Fig. 9A–C) presumably because varying age control and sample density led to misalignment and averaging of the short-term events, as well as small geographic differences in the rates, timing, and causes of local changes in vegetation composition. Also, the climate changes may not have been abrupt at all sites.

A map of the thermal-preference reconstructions (Fig. 10) shows that the difference between 7 ka and 5 ka would be consistent with coastal cooling. The vegetation preferences suggest July temperatures could have decreased by 0.1–1.0 °C at coastal sites, but could have increased by 0.1–1.8 °C at inland sites.

3.4.2. Comparison with paleoceanographic datasets

The sharp decline in the mean July temperature preference of the coastal vegetation from 22 to 19.5 °C by 5.0 ka appears consistent with >1 °C decrease in alkenone-reconstructed SSTs off the coast of Nova Scotia (Fig. 9A), as well as other indications of oceanic changes at this time, such as a reduction in North Atlantic Deepwater production noted by a negative carbon-isotopic excursion in benthic foraminifera and a change in North Atlantic Gyre circulation inferred from planktonic foraminifera (Oppo et al., 2003; Sachs, 2007; Thornalley et al., 2009). Foraminifera-inferred SSTs off the coast of West Africa (deMenocal et al., 2000) further indicate that the cooling off Nova Scotia was not limited to a small portion of the Atlantic, but involved both the Labrador and Canary Currents on opposite sides of the gyre.

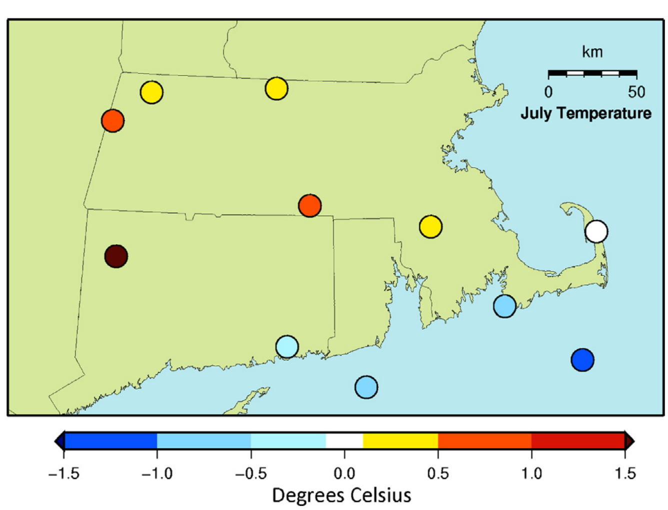

Fig. 10. Difference map for July temperature at all coastal and inland sites showing reconstructed changes between 7 and 5 ka (5 ka minus 7 ka). Warm colors indicate a positive change, with cool colors indicating a negative change. (For interpretation of the references to color in this figure legend, the reader is referred to the web version of this article.)

4. Discussion

4.1. Reconstruction similarities and their implications

Many of the lake-level changes interpreted from stratigraphic units at Deep Pond correspond with similar evidence of lake-level changes at Davis and Crooked Ponds, MA (Newby et al., 2009, 2011; Shuman et al., 2001, 2009) as well as other sites in the region (see discussion of the comparison of New Long Pond, MA and White Pond, NJ with Davis Pond in Newby et al., 2011). All of these sites experienced brief episodes of low water recorded by sand layers in intermediate depth cores at ca 5.5 ka (e.g., Fig. 8B).

All of the records also record a long-term water-level rise consistent with the long-term increase in pollen-inferred vegetation precipitation requirements (Fig. 8A). The long-term rise in the lake-level reconstruction (Fig. 7) does not appear to represent a bias related to sediment infilling or other intrinsic aspects of lake development because records in other regions (e.g., in New Hampshire; Wyoming) show the opposite pattern with extensive sediments associated with early phases of high water (Davis and Ford, 1982; Shuman et al., 2005, 2010; Minckley et al., 2012).

The correlations among the $\Delta P\text{–}E$ (lake-level) and vegetation precipitation-requirement reconstructions at Deep Pond and throughout the region indicate that the vegetation history tracked changes in effective moisture that also produced stratigraphically-meaningful lake-level changes. A dynamic moisture–vegetation equilibrium (c.f. Webb, 1986) appears to have persisted even during the hemlock decline. The agreement between the lake-level and pollen data confirms that reduced effective moisture likely contributed to the prolonged period of low hemlock abundance, even at coastal sites, particularly given evidence of brief episodes of recovery that were truncated by subsequent dry episodes (Fig. 8).

Likewise, the similarities between SST data and coastal temperature-preference reconstructions (Fig. 9A) indicate a likely dynamic equilibrium between temperature and vegetation. As confirmed by the temperature preference reconstructions, coastal cooling of ~1 °C could explain the rapid replacement of oak by pine and beech. Inland temperatures cannot be independently constrained, but an increase in inland temperatures could have resulted from reduced latent heating during periods of drought.

Some moderate-to-low correlation coefficients between the independent climate and the vegetation-requirement reconstructions (Table 1) may be related to the low temporal resolution and low numbers of radiocarbon ages constraining the details of some records. Additionally, uncertainty in the reconstructions, landscape-scale spatial differences in climate, and superimposed ecological factors (e.g., frequent fire at sites like Duck Pond) likely also contribute to the differences. For example, if Duck Pond experienced frequent burning, it may have limited the establishment of equilibrium between vegetation and moisture (see e.g., Green, 1982; Minckley et al., 2012).

4.2. Paleoclimate controls

In summary, the lake-level and pollen data indicate region-wide, ecologically significant drought after 5.5 ka, which may have coincided with coastal cooling and inland warming. While drought and temperature change likely contributed to the changes in hemlock and oak abundance (Foster et al., 2006), pests and pathogens (Allison et al., 1986; Anderson et al., 1986; Bhiry and Filion, 1996), wind throw (Busby et al., 2009), and fires and human activity (Fuller et al., 1998) cannot be ruled out as important factors influencing the vegetation (and pollen-inferred temperature gradients) in the context of regional drought that lowered lake levels. Likewise, modern spatial correlations between temperature and precipitation, embedded in the use of modern analogs, complicate our ability to accurately infer climate changes that likely changed the spatial correlations.

However, if climate changes at 5.5 ka produced a shift in the inland-coastal temperature gradient, inland warming and drought may have resulted from atmospheric circulation changes and oceanic variability. If so, non-linear oceanic responses to slow orbital changes likely contributed to the changes across southern New England. The 1 °C decline in SSTs measured off the coasts of Nova Scotia and Virginia (Sachs, 2007) at ca 5.5 ka is interpreted as an intensification and southward shift of the Labrador Current, and would be consistent with the type of coastal circulation changes that triggered the severe AD 1965 drought in the northeast U.S. (Namias, 1966). Kim et al. (2007) find abrupt cooling by ca 5.5 ka in the first EOF of North Atlantic alkenone records consistent with the foraminifera-inferred SST record off the coast of west Africa (deMenocal et al., 2000) and an abrupt shift in gyre circulation (rotating ocean currents) spanning the entire North Atlantic (e.g., Thornalley et al., 2009). Changes in both the Canary and Labrador Current could reflect circulation and thermocline adjustments related to changes in the Atlantic Meridional Overturning Circulation (AMOC) (Oppo et al., 2003; Thornalley et al., 2009).

In this scenario, an abrupt change within the ocean system would produce changes in the pressure and wind fields across the Atlantic that influence precipitation in the northeast U.S. consistent with oxygen-isotope changes at 5.5 ka in a record from Fayetteville Green Lake, NY (Kirby et al., 2002). The negative oxygen-isotope excursion at ca 5.5 ka indicates changed storm tracks, a weakened Atlantic subtropical high, and resulting alteration of precipitation production and delivery.

5. Conclusions

The hemlock decline represents the most abrupt vegetation change of the Holocene in eastern North America, and although extensively studied, it remains poorly understood. Evidence of a synchronous oak decline, and beech and pine increases at coastal Massachusetts, raise questions about potential climatic drivers of these extensive vegetation changes. Even if climate did not cause the declines, our results provide support for the interpretation that drought helped to maintain the subsequent period of low hemlock and oak abundance. The correlation between the lake-level and vegetation precipitation-requirement histories, as well as brief periods of recovery by hemlock during wet periods, indicates a dynamic equilibrium between vegetation and effective moisture at century to millennial scales.

Our lake-level reconstruction from a coastal site, Deep Pond, shows that moisture–hemlock relationships did not differ meaningfully across the northeastern U.S. despite the vegetation differences between coastal and inland sites. The vegetation composition tracked the moisture variations closely in both areas, but MAT temperature-preference reconstructions indicate that coastal cooling, consistent with a 1 °C decline in coastal SSTs, could explain why the coastal oak decline and beech increase is not observed inland. Based on these results, a modified ocean–atmosphere system, which caused the Labrador Current to intensify south past Cape Cod and altered delivery of precipitation in the northeastern United States, could be the ultimate driver of the hemlock decline and related changes.

Acknowledgments

This work was supported by National Science Foundation grants to Shuman (DEB-0816731) and Foster and Oswald (DEB-0815036). We also thank S.T. Jackson, P. Heller, T.A. Minckley, B.R. Marsicek, J.L.

Gill, and three anonymous reviewers for helpful comments that greatly improved the manuscript; G.E. Carter, J. Calder, J. Donnelly, P. Pribyl, T. Miller, and D. Colvard for field and lab assistance; D.J. Marsicek and L.A. Marsicek for moral support.

Appendix I. Quantitative lake-level and moisture-balance reconstructions

Small lakes (such as Deep Pond) are ideal sites for generating quantitative effective moisture reconstructions if they have no surface inlets or outlets because changes in lake volume can be related to the balance of precipitation and evaporation across the watershed (Harrison and Digerfeldt, 1993; Plank and Shuman, 2009; Shuman et al., 2010). To generate a quantitative reconstruction here, we systematically identify littoral and transitional (sublittoral) sediments within the cores (based on core data interpolated to 50-yr time steps for comparison in time across cores). We do so to constrain the elevation of the sediment limit through time (Fig. 3), and use LOI thresholds that distinguish the different facies.

Littoral sediments were assumed to have less than 20–45% LOI, and transitional sediments to have less than 65–75% LOI. To account for uncertainty in knowing the threshold values for the past, we repeated our facies classifications 18 times using a single value (e.g., 35% and 75%) for the upper LOI limits of littoral and transitional facies in each iteration. We modified both limits by 5 percentage points between iterations in combination: six 5% steps for the littoral limit times three 5% steps for the transitional limit produced the 18 iterations.

To represent the elevation of the sediment limit (and thus the paleoshoreline) over time, we average the minimum elevations of the littoral and transitional sediments in any of the cores per 50-yr interval because these elevations bracket the position of the sediment limit. We assume that the magnitude of the changes in elevation of the sediment limit equal the magnitude of changes in the lake surface elevation (ΔElev).

Having generated a quantitative time series of lake elevation, we use a simple mass-balance approach outlined by Shuman et al. (2010) to reconstruct effective moisture within the watershed. Precipitation (P) and evapotranspiration (E) cannot be measured individually, so we quantify them in this paper as one variable ($\Delta P\text{–}E$):

$$\Delta P - E = \Delta V_L/(A_W{*}\Delta T) = (\Delta \mathrm{Elev}{*}A_L)/(A_W{*}\Delta T) \quad (1)$$

The approach first uses the surface area of the lake ($A_L = 8{,}925\ \mathrm{m}^2$) and the lake-elevation changes (ΔElev; estimated as the reconstructed changes in the elevation of the sediment limit) to approximate the changes in lake volume (ΔV_L). Then, we use ΔV_L with the area of the watershed ($A_W = 84{,}677\ \mathrm{m}^2$) and a range of lake-climate equilibration times consistent with estimates for hydrologically open lakes ($\Delta T = 0.5\text{–}5$ years; after Mason et al., 1994) to quantitatively reconstruct $\Delta P\text{–}E$. ΔT refers to how quickly lake volume integrates changes in precipitation and evaporation over the catchment area (Mason et al., 1994).

ΔElev is used here rather than the change in lake depth because sediment infilling monotonically reduces depth independent of climate, and depth also depends on a large volume of water unaffected by changes in climate (i.e., retained in the lake even at its lowest level). ΔElev represents the reduction or addition of a near-surface volume of water associated with changes in precipitation and evapotranspiration across the watershed (see Plank and Shuman, 2009).

This approach relies on a couple of simplifications before we can estimate $\Delta P\text{–}E$. We ignore changes in 1) the lake bathymetry due to infilling and 2) the volume of watershed groundwater. Both assumptions relate to the lake as a surficial expression of the groundwater table, which has a climatically-controlled elevation. We ignore infilling because sediment infilling only affects the periphery of the volume of water associated with lake-level (water-table level) changes (ΔV_L). Infilling can significantly reduce water depths and volumes in the center of the lake, but this area always remains saturated below even the lowest water-table levels during droughty periods and is not relevant to estimating ΔElev, ΔV_L, or $\Delta P\text{–}E$ (see Plank and Shuman, 2009). Additionally, because most lake sediments have high water contents (>75%), the total water volume displaced by sediment and the effect on $\Delta P\text{–}E$ is small (~2%, see calculations by Pribyl and Shuman, in review).

We do not account for changes in the volume of shallow groundwater in the watershed, even though water-table changes are likely equal in magnitude to the lake-level changes, because the continuity of the local groundwater is not known. Because changes to the bathymetry would likely modestly reduce $\Delta P\text{–}E$ estimates, but changes in the water-table elevation would likely increase $\Delta P\text{–}E$ (by increasing ΔV_L), we assume that our $\Delta P\text{–}E$ estimates are underestimates.

To account for other uncertainties in our $\Delta P\text{–}E$ calculations for Deep Pond, we repeated Eq. (1) with multiple sets of inputs. The different inputs include a range of estimates of ΔV_L based on a) the ensemble of ΔElev reconstructions produced using the 18 different LOI thresholds for defining the sediment limit, and b) the uncertainties in ΔElev related to our inability to know the position of the sediment limit between cores. Accordingly, we calculated $\Delta P\text{–}E$ using three estimates of ΔV_L, which were based on the means of 1) the 18 ΔElev reconstructions, 2) the equivalent 18 reconstructions of the maximum possible ΔElev allowed by the core spacing (based on the minimum elevation of transitional sediments, or the lower constraint on the position of the sediment limit, through time), and 3) 18 minimum possible values of ΔElev allowed by the core spacing (based on the minimum elevation of littoral sediments, or the upper constraint on the position of the sediment limit, through time). For each value of ΔV_L, we applied 50 different values of ΔT, the lake-climate equilibration time in Eq. (1), which were evenly distributed between 0.5 and 5 years based on a compilation of values for modern lakes (Mason et al., 1994). Consequently, the mean and uncertainty in our reconstruction represent 150 different calculations of Eq. (1) for each 50-yr time step.

References

Allison, T.D., Moeller, R.E., Davis, M.B., 1986. Pollen in laminated sediments provides evidence for a mid-Holocene forest pathogen outbreak. Ecology 67, 1101–1105.

Anderson, R.S., Davis, R.B., Miller, N.G., Stuckenrath, R., 1986. History of late-and post-glacial vegetation and disturbance around Upper South Branch Pond, northern Maine. Can. J. Bot. 64, 1977–1986.

Baker, G.S., Jordan, T.E., Pardy, J., 2007. An Introduction to Ground Penetrating Radar (GPR). The Geological Society of America Special Paper 432, pp. 1–18.

Bartlein, P.J., Harrison, S.P., Brewer, S., Connor, S., Davis, B.A.S., Gajewski, K., Guiot, J., Harrison-Prentice, T.I., Henderson, A., Peyron, O., Prentice, I.C., Scholze, M., Seppa, H., Shuman, B., Sugita, S., Thompson, R.S., Viau, A.E., Williams, J., Wu, H., 2010. Pollen-based continental climate reconstructions at 6 and 21 ka: a global synthesis. Clim. Dyn. 35. http://dx.doi.org/10.1007/s00382-010-0904-1.

Bennett, K.D., Fuller, J.L., 2002. Determining the age of the mid-Holocene *Tsuga canadensis* (hemlock) decline, eastern North America. Holocene 12, 421–429.

Bhiry, N., Filion, L., 1996. Mid-Holocene hemlock decline in eastern North America linked with phytophagous insect activity. Quat. Res. 45, 312–320.

Booth, R.K., Brewer, S., Blauuw, M., Minckley, T.A., Jackson, S.T., 2012. Decomposing the mid-Holocene *Tsuga* decline in eastern North America. Ecology 93 (8), 1841–1852.

Busby, P.E., Canham, C.D., Motzkin, G., Foster, D.R., 2009. Forest response to chronic hurricane disturbance in coastal New England. J. Veg. Sci. 20, 487–497.

Calcote, R., 2003. Mid-Holocene climate and the hemlock decline: the range limit of *Tsuga canadensis* in the western Great Lakes region, USA. Holocene 13, 215–224.

Davis, M.B., 1969. Climatic changes in southern Connecticut recorded by pollen deposition at Rogers Lake. Ecology 50, 409–422.

Davis, M.B., 1981. Outbreaks of forest pathogens in Quaternary history. In: Proceedings of the Fourth International Palynological Conference 3: Lucknow, India, pp. 216–227.
Davis, M.B., Ford, M.S., 1982. Sediment focusing in Mirror Lake, New Hampshire. Limnol. Oceanogr. 27, 137–150.
Dearing, J.A., 1997. Sedimentary indicators of lake-level changes in the humid temperate zone: a critical review. J. Paleolimnol. 18, 1–14.
deMenocal, P., Ortiz, J., Guilderson, T., Adkins, J., Sarnthein, M., Baker, L., Yarusinsky, M., 2000. Abrupt onset and termination of the African Humid Period: rapid climate responses to gradual insolation forcing. Quat. Sci. Rev. 19, 347–361.
Digerfeldt, G., 1986. Studies on past lake-level fluctuations. In: Berglund, B.E. (Ed.), Handbook of Holocene Palaeoecology and Palaeohydrology. John Wiley & Sons, New York, pp. 127–143.
Dunwiddie, P.W., 1990. Postglacial vegetation history of coastal islands in southeastern New England. Natl. Geogr. Res. 6, 178–195.
Foster, D.R., Oswald, W.W., Faison, E.K., Doughty, E.D., Hansen, B.C.S., 2006. A climatic driver for abrupt mid-Holocene vegetation dynamics and the hemlock decline in New England. Ecology 87, 2959–2966.
Fuller, J.L., Foster, D.R., McLachlan, J.S., Drake, N., 1998. Impact of human activity on regional forest composition and dynamics in central New England. Ecosystems 1, 76–95.
Gaudreau, D.C., 1986. Late-quaternary Vegetational History of the Northeast: Paleoecological Implications of Topographic Patterns in Pollen Distributions (PhD thesis). Yale University, New Haven, CT, USA.
Green, D.G., 1982. Fire and stability in the postglacial forests of southwest Nova Scotia. J. Biogeogr. 9, 29–40.
Grimm, E.C., Maher Jr., L.J., Nelson, D.M., 2009. The magnitude of error in conventional bulk-sediment radiocarbon dates from central North America. Quat. Res. 72, 301–308.
Guiot, J., Harrison, S.P., Prentice, I.C., 1993. Reconstruction of Holocene precipitation patterns in Europe using pollen and lake-level data. Quat. Res. 40, 139–149.
Haas, J.N., McAndrews, J.H., 1999. The summer drought related hemlock (Tsuga canadensis) decline in Eastern North America 5700 to 5100 years ago. In: McManus, K. (Ed.), Symposium on Sustainable Management of Hemlock Ecosystems in Eastern North America, Volume Durham. United States Department of Agriculture, Forest Service, Northeastern Research Station, New Hampshire, p. 81. General Technical Report NE-267.
Harrison, S.P., Digerfeldt, G., 1993. European lakes as palaeohydrological and palaeoclimatic indicators. Quat. Sci. Rev. 12, 233–248.
Heiri, O., Lotter, A.F., Lemcke, G., 2001. Loss on ignition as a method for estimating organic and carbonate content in sediments: reproducibility and comparability of results. J. Paleolimnol. 25, 101–110.
Kim, J.-H., Meggers, H., Rimbu, N., Lohmann, G., Freudenthal, T., Muller, P.J., Schneider, R.R., 2007. Impacts of the North Atlantic gyre circulation on Holocene climate off northwest Africa. Geology 35 (5), 387–390.
Kirby, M.E., Mullins, H.T., Patterson, W.P., Burnett, A.W., 2002. Late glacial-Holocene atmospheric circulation and precipitation in the northeast United States inferred from modern calibrated stable oxygen and carbon isotopes. Geol. Soc. Am. Bull. 114, 1326–1340.
Lavoie, M., Richard, P.J.H., 2000. Postglacial water-level changes of a small lake in southern Quebec, Canada. Holocene 10, 621–634.
Mason, I.M., Guzkowska, M.A.J., Rapley, C.G., Street-Perrott, F.A., 1994. The response of lake levels and areas to climatic change. Clim. Change 27, 161–197.
Minckley, T.A., Shriver, R.K., Shuman, B.N., 2012. Resilience and regime change in a southern Rocky Mountain ecosystem during the past 17000 years. Ecol. Monogr. 82 (1), 49–68.
Moorman, B.J., 2001. Ground-penetrating radar applications in paleolimnology. In: Last, W.M., Smol, J.P. (Eds.), Tracking Environmental Change Using Lake Sediments: Physical and Chemical Techniques. Kluwer Academic Publishers, Dordrecht, The Netherlands, pp. 1–25.
Muller, S.D., Richard, P.J.H., Guiot, J., de Beaulieu, J.L., Fortin, D., 2003. Postglacial climate in the St. Lawrence lowlands, southern Quebec: pollen and lake-level evidence. Palaeogeogr. Palaeoclimatol. Palaeoecol. 193, 51–72.
Namias, J., 1966. Nature and possible causes of the northeastern United States drought during 1962–65. Mon. Weather Rev. 94, 543–554.
Nelson, D.M., Hu, F.S., Grimm, E.C., Curry, B.B., Slate, J.E., 2006. The influence of aridity and fire on Holocene prairie communities in the eastern Prairie Peninsula. Ecology 87 (10), 2523–2536.
Newby, P.C., Killoran, P., Waldorf, M., Shuman, B., Webb III, T., Webb, R.S., 2000. 14,000 years of sediment, vegetation, and water level changes at Makepeace Cedar Swamp, southeastern Massachusetts. Quat. Res. 53, 352–368.
Newby, P.E., Donnelly, J.P., Shuman, B.N., MacDonald, D., 2009. Evidence of centennial-scale drought from southeastern Massachusetts during the Pleistocene/Holocene transition. Quat. Sci. Rev. 28, 1675–1692.
Newby, P.E., Shuman, B.N., Donnelly, J.P., MacDonald, D., 2011. Repeated century-scale droughts over the 13,000 yr near the Hudson River watershed, USA. Quat. Res. 75, 523–530.
Oldale, R.N., 1992. Cape Cod and the islands: the Geologic Story. Parnass. Impr., 126–128.
Oppo, D.W., McManus, J.F., Cullen, J.L., 2003. Deepwater variability in the Holocene epoch. Nature 422, 277–278.
Oswald, W.W., Anderson, P.M., Brown, T.A., Brubaker, L.B., Hu, F.S., Lozhkin, A.V., Tinner, W., Kaltenrieder, P., 2005. Effects of sample mass and macrofossil type on radiocarbon dating of arctic and boreal lake sediments. Holocene 15, 758–767.
Oswald, W.W., Faison, E.K., Foster, D.R., Doughty, E.D., Hansen, B.C.S., 2007. Postglacial changes in spatial patterns of vegetation across southern New England. J. Biogeogr. 34, 900–913.
Overpeck, J.T., Webb III, T., Prentice, I.C., 1985. Quantitative interpretation of fossil pollen spectra: dissimilarity coefficients and the method of modern analogs. Quat. Res. 23, 87–108.
Parnell, A.C., Haslett, J., Allen, J.R.M., Buck, C.E., Huntley, B., 2008. A flexible approach to assessing synchroneity of past events using Bayesian reconstructions of sedimentation history. Quat. Sci. Rev. 27, 1872–1885.
Plank, C., Shuman, B., 2009. The effects of lake area and volume changes on the surface energy budget of Minnesota's lake-dotted landscape. J. Clim. 22, 4055–4065.
Pribyl, P., Shuman, B. A Computational Approach to Quaternary Lake-Level Reconstruction Applied to Lake of the Woods, Wyoming, USA. Quat. Res. (in review).
Reimer, P.J., Baillie, M.G.L., Bard, E., Bayliss, A., Beck, J.W., Blackwell, P.G., Bronk Ramsey, C., Buck, C.E., Burr, G.S., Edwards, R.L., Friedrich, M., Grootes, P.M., Guilderson, T.P., Hajdas, I., Heaton, T.J., Hogg, A.G., Hughen, K.A., Kaiser, K.F., Kromer, B., McCormac, F.G., Manning, S.W., Reimer, R.W., Richards, D.A., Southon, J.R., Talamo, S., Turney, C.S.M., van der Plicht, J., Weyhenmeyer, C.E., 2009. INTCAL09 and MARINE09 radiocarbon age calibration curves, 0–50,000 years cal BP. Radiocarbon 51 (4), 1111–1150.
Sachs, J.P., 2007. Cooling of Northwest Atlantic slope waters during the Holocene. Geophys. Res. Lett. 34, L03609.
Shane, L.C.K., Anderson, K.H., 1993. Intensity, gradients and reversals in late glacial environmental change in east-central North America. Quat. Sci. Rev. 12, 307–320.
Shuman, B., 2003. Controls on loss-on-ignition variation in cores from two shallow lakes in the northeastern United States. J. Paleolimnol. 30, 371–385.
Shuman, B., Bravo, J., Kaye, J., Lynch, J.A., Newby, P., Webb III, T., 2001. Late- Quaternary water-level variations and vegetation history at Crooked Pond, southeastern Massachusetts. Quat. Res. 56, 401–410.
Shuman, B., Newby, P., Huang, Y., Webb III, T., 2004. Evidence for the close climatic control of New England vegetation history. Ecology 85, 1297–1310.
Shuman, B., Newby, P., Donnelly, J.P., Tarbox, A., Webb III, T., 2005. A record of late-Quaternary moisture-balance change and vegetation response from the White Mountains, New Hampshire. Ann. Assoc. Am. Geogr. 95, 237–248.
Shuman, B.N., Newby, P., Donnelly, J.P., 2009. Abrupt climate change as an important agent of ecological change in the Northeast U.S. throughout the past 15,000 years. Quat. Sci. Rev. 28, 1693–1709.
Shuman, B., Pribyl, P., Minckley, T.A., Shinker, J.J., 2010. Rapid hydrologic shifts and prolonged droughts in Rocky Mountain headwaters during the Holocene. Geophys. Res. Lett. 37, L06701.
Suter, S.M., 1985. Late-glacial and Holocene vegetation history in southeastern Massachusetts: a 14,000-year pollen record. Curr. Res. Pleistocene 2, 87–89.
Telford, R.J., Birks, H.J.B., 2005. The secret assumption of transfer functions: problems with spatial autocorrelation in evaluation model performance. Quat. Sci. Rev. 24, 2173–2179.
Thornalley, D.J.R., Elderfield, H., McCave, I.N., 2009. Holocene oscillations in temperature and salinity of the surface subpolar North Atlantic. Nature 457, 711–714.
Tzedakis, P.C., 1992. Effects of soils on the Holocene history of forest communities, Cape Cod Massachusetts, U.S.A. Géogr. Phys. Quat. 46, 113–124.
Webb III, T., 1986. Is vegetation in equilibrium with climate? How to interpret late-Quaternary pollen data. Vegetatio 67 (2), 75–91.
Webb, R.S., Anderson, K.H., Webb III, T., 1993. Pollen response-surface estimates of late-Quaternary changes in the moisture balance of the northeastern United States. Quat. Res. 40, 213–227.
Whitehead, D.R., 1979. Late-glacial and post-glacial vegetational history of the Berkshires, western Massachusetts. Quat. Res. 3, 333–357.
Whitehead, D.R., Crisman, T.L., 1978. Paleolimnological studies of small New England (U.S.A.) ponds. Part I. Late-glacial and post-glacial tropic oscillations. Pol. Arch. Hydrobiol. 25, 471–481.
Whitmore, J., Gajewski, K., Sawada, M., Williams, J.W., Shuman, B., Bartlein, P.J., Minckley, T., Viau, A.E., Webb III, T., Shafer, S., Anderson, P., Brubaker, L., 2005. Modern pollen data from North America and Greenland for multi-scale paleoenvironmental applications. Quat. Sci. Rev. 24, 1828–1848.
Williams, A.S., 1974. Late-glacial – Postglacial Vegetational History of the Pretty Lake Region, Northeastern Indiana. U.S. Geological Survey Professional Paper 686, p. 23.
Williams, J.W., Shuman, B., 2008. Obtaining accurate and precise environmental reconstructions from the modern analog technique and North American surface pollen dataset. Quat. Sci. Rev. 27, 669–687.
Williams, J.W., Shuman, B.N., Webb III, T., Bartlein, P.J., Leduc, P.L., 2004. Late-Quaternary vegetation dynamics in North America: scaling from taxa to biomes. Ecol. Monogr. 74, 309–334.
Winkler, M.G., 1985. A 12,000-year history of vegetation and climate for Cape Cod, Massachusetts. Quat. Res. 23, 301–312.
Wright Jr., H.E., 1967. A square-rod piston sampler for lake sediments. J. Sediment. Petrol. 27, 957–976.
Yu, Z., McAndrews, J.H., Eicher, U., 1997. Middle Holocene dry climate caused by change in atmospheric circulation patterns: evidence from lake levels and stable isotopes. Geology 25, 251–254.